Protein Science (1993), *2*, 985–1000. Cambridge University Press. Printed in the USA.

Disulfide bonds in homo- and heterodimers of EF-hand subdomains of calbindin D_{9k}: Stability, calcium binding, and NMR studies

SARA LINSE, EVA THULIN, AND PETER SELLERS

Physical Chemistry 2, Lund University, Chemical Center, S-221 00 Lund, Sweden

(RECEIVED December 21, 1992; REVISED MANUSCRIPT RECEIVED February 18, 1993)

Abstract

The effect of decreased protein flexibility on the stability and calcium binding properties of calbindin D_{9k} has been addressed in studies of a disulfide bridged calbindin D_{9k} mutant, denoted (L39C + P43M + I73C), with substitutions Leu 39 → Cys, Ile 73 → Cys, and Pro 43 → Met. Backbone ^{1}H NMR assignments show that the disulfide bond, which forms spontaneously under air oxidation, is well accommodated. The disulfide is inserted on the opposite end of the protein molecule with respect to the calcium sites, to avoid direct interference with these sites, as confirmed by ^{113}Cd NMR. The effect of the disulfide bond on calcium binding was assessed by titrations in the presence of a chromophoric chelator. A small but significant effect on the cooperativity was found, as well as a very modest reduction in calcium affinity. The disulfide bond increases T_m, the transition midpoint of thermal denaturation, of calcium free calbindin D_{9k} from 85 to 95 °C and C_m, the urea concentration of half denaturation, from 5.3 to 8.0 M. Calbindins with one covalent bond linking the two EF-hand subdomains are equally stable regardless if the covalent link is the 43–44 peptide bond or the disulfide bond.

Kinetic remixing experiments show that separated CNBr fragments of (L39C + P43M + I73C), each comprising one EF-hand, form disulfide linked homodimers. Each homodimer binds two calcium ions with positive cooperativity, and an average affinity of 10^6 M^{-1}. Disulfide linkage dramatically increases the stability of each homodimer. For the homodimer of the C-terminal fragment T_m increases from 59 ± 2 without covalent linkage to 91 ± 2 °C with disulfide, and C_m from ≈1.5 to 7.5 M. The overall topology of this homodimer is derived from ^{1}H NMR assignments and a few key NOEs.

Keywords: calbindin; calcium binding; cooperativity; disulfide; EF-hand; flexibility; NMR; stability

Disulfide bonds can have a pronounced effect on the stability of the folded structure of a protein. There are numerous reports of effects on protein stability of a second, third, or more covalent bond linking different parts of the polypeptide chain. The net effect varies widely and incorporation of a disulfide bond does not necessarily lead to increased stability (for review see Matsumura & Matthews, 1991; Tidor & Karplus, 1993). Studies of the effect of disulfide bonds on other properties than protein stability have been less extensive. Some recent investigations show that enzymatic action can be either facilitated or hindered by an SS-bond which increases the stability and reduces the flexibility of the protein (Habuka et al., 1991; Kruse et al., 1991; Uchida et al., 1991; Day et al., 1992).

Some proteins in the calmodulin superfamily (Kretsinger, 1987; Strynadka & James, 1991) of calcium binding proteins contain one or more cysteine residues, e.g., calbindin D_{28k}, troponin C, and S-100β. However, most members of this superfamily do not have naturally occurring disulfides, e.g., calmodulin, TnC, and calbindin D_{9k}. Insertion of non-native disulfides has therefore been a successful strategy for studying the role of the conformational switch accompanying Ca^{2+} binding to EF-hand pair domains of regulatory calcium binding proteins (Grabarek et al., 1990, 1991). Disulfides that favor the

Reprint requests to: Sara Linse, Physical Chemistry 2, Lund University, Chemical Center, P.O. Box 124, S-221 00 Lund, Sweden.

Abbreviations: TnC, troponin C; CaM, calmodulin; DTT, dithiothreitol; TFA, trifluoroacetic acid; quin 2, 2-[[2-[bis(carboxymethyl) amino]-5-methylphenoxy]methyl]-6-methoxy-8-[bis(carboxymethyl) amino]-quinoline; 5,5′-Br_2-BAPTA, 5,5′-dibromo-1,2-bis(*o*-aminophenoxy)-ethane-*N*,*N*,*N*′,*N*′-tetraacetic acid; COSY, J-correlated spectroscopy; R-COSY, relayed COSY; TOCSY, total correlation spectroscopy; NOE, nuclear Overhauser effect; NOESY, NOE spectroscopy.

calcium free conformations of TnC and CaM were found to lower the calcium affinity and inhibit activation of various enzymes (Grabarek et al., 1990, 1991).

Calbindin D_{9k} is a small (75 amino acids) and highly stable protein with two EF-hands that bind calcium with high affinity and positive cooperativity. Solution (Kördel et al., 1993) and crystal (Szebenyi & Moffat, 1986; Svensson et al., 1992) structures of calcium loaded calbindin D_{9k} have been determined to high resolution and are highly similar. In contrast to the calcium-regulatory proteins calmodulin and troponin C, the conformational changes accompanying calcium binding to calbindin D_{9k} are very subtle (Skelton et al., 1990). However, the calcium-induced changes in dynamics are profound (Linse et al., 1990; Skelton et al., 1990, 1992). The molecular events underlying the cooperativity of calcium binding to calbindin D_{9k} are also starting to be unraveled. In a recent study involving negatively charged residues in the vicinity of the Ca^{2+} binding sites, but not directly coordinating the calcium ions, it was found that some of these charges play a crucial role not only for the Ca^{2+} affinity but also for the cooperativity (Linse et al., 1991). A complementary approach involving the structure and dynamics of a calbindin D_{9k} species with cadmium occupying only one of the sites (Akke et al., 1991; Skelton et al., 1992) has indicated that reduction of the flexibility of both EF-hands which is most pronounced on binding the first ion is another component in the mechanism of the cooperativity.

In all of the naturally occurring EF-hand pair domains studied so far, the two EF-hands have somewhat different sequences. These domains can therefore be viewed as covalently linked heterodimers of EF-hands. A recently evolving approach to the understanding of calcium binding to EF-hands has been to produce peptide fragments comprising only one EF-hand (Reid et al., 1990; Shaw et al., 1990; Tsuji, 1991; Finn et al., 1992). It appears that, in the presence of calcium, the isolated EF-hand is unfavored and instead a homodimer is the observed species (Shaw et al., 1990, 1992; Kay et al., 1991; Finn, 1992).

The aim of the present work is to investigate the role of protein flexibility in the stability and calcium binding properties of recombinant bovine calbindin D_{9k} by insertion of a disulfide bond. Cysteines were substituted for Leu 39 and Ile 73, and methionine for Pro 43, to yield the triple mutant (L39C + P43M + I73C). Residues 39 and 73 were selected because the crystal coordinates indicate that cysteines in these positions can form a disulfide bond of near optimal geometry with only minor rearrangement of the protein and because they are located on the opposite end of the protein with respect to the calcium sites (cf. Fig. 1). The engineered disulfide is hence not likely to interfere directly with the calcium sites. It would thus be suitable for probing the role of changes in large scale dynamics involving the entire protein in the cooperativity of calcium binding. The substitution of methionine for Pro 43 makes it possible to cleave (by CNBr) the protein into two fragments comprising the first and second EF-hand, respectively (Finn et al., 1992). It has therefore been possible to compare the stability of a protein with zero, one or two covalent bonds linking two halves, i.e., with none, one, or both of the 43–44 peptide bond and the 39–73 disulfide bond linking the two EF-hand subdomains. The present work also encompasses stability and calcium binding studies of disulfide linked homodimers of each CNBr fragment of (L39C + P43M + I73C). Almost complete assignments are presented for one of the homodimers. The positions of the disulfides in the two homodimers are not equivalent; residue 73 is within helix IV, whereas residue 39 is outside of helix II, which ends at position 36. The influence of this difference on the stability properties of the two homodimers will be discussed.

Nomenclature for proteins and fragments

The same residue numbering as in wild-type recombinant bovine minor A calbindin D_{9k} (see Linse et al., 1987) is used throughout.

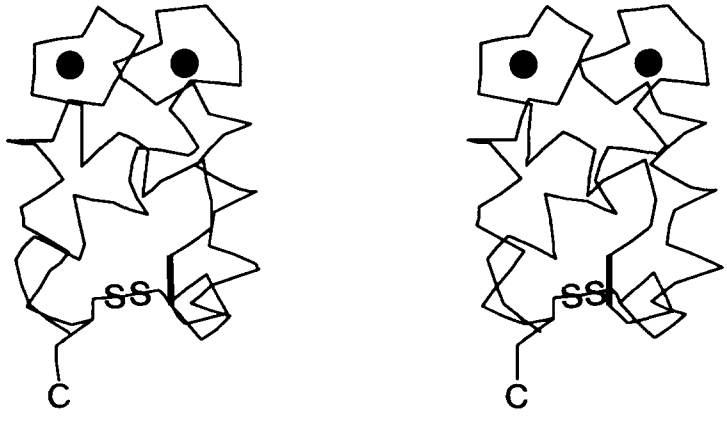

Fig. 1. Stereo view of α-carbon structure of calbindin D_{9k} mutant (L39C + P43M + I73C), based on the crystal structure of bovine calbindin D_{9k}. The location of the 39–73 disulfide bond is indicated with SS and the 43–44 connection with a thicker line. Filled circles indicate calcium ions.

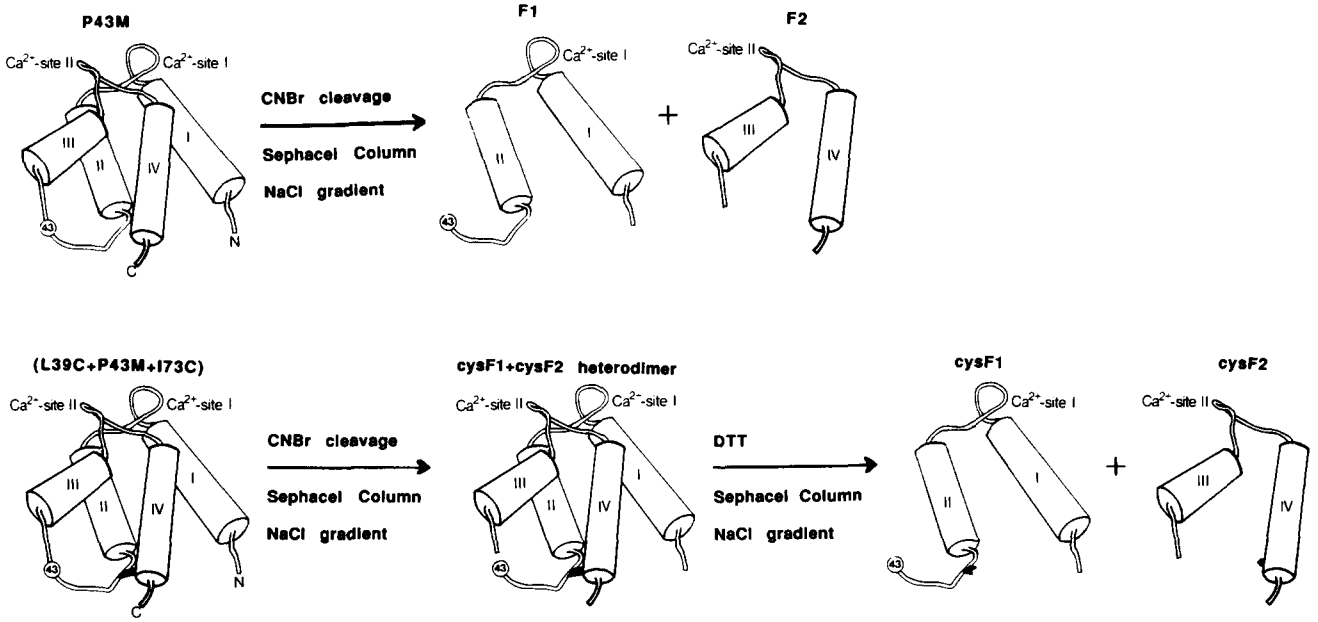

Fig. 2. Nomenclature of proteins and fragments. The figure also illustrates the results of CNBr cleavage and separation on an ion exchange column in the presence of EDTA.

(L39C + P43M + I73C), calbindin D_{9k} mutant, with the substitutions Leu 39 → Cys, Pro 43 → Met, and Ile 73 → Cys

P43M, mutant with the substitution Pro 43 → Met

cysF1, fragment comprising residues 1–43 of (L39C + P43M + I73C), thus including Ca^{2+} site I

cysF2, fragment comprising residues 44–75 of (L39C + P43M + I73C), thus including Ca^{2+} site II

F1, fragment comprising residues 1–43 of P43M

F2, fragment comprising residues 44–75 of P43M

heterodimer, complex comprising residues 1–43 plus residues 44–75; the term heterodimer can, with this general definition, refer to (L39C + P43M + I73C), P43M, or a complex of one of F1 or cysF1 and one of F2 or cysF2

The nomenclature is also explained by schematic drawings of calcium-free proteins and fragments in Figure 2. The sequences of cysF1 and cysF2 are shown in Table 1, in which positions corresponding to calcium ligand coordinates in intact calbindin D_{9k} are highlighted.

Definition of Ca^{2+} binding constants and cooperativity

Microscopic (or site) binding constants have Roman subscripts.

K_I, binding constant of site I when site II is empty

K_{II}, binding constant of site II when site I is empty

$K_{I,II}$, binding constant of site I when site II has bound Ca^{2+}

$K_{II,I}$, binding constant of site II when site I has bound Ca^{2+}

Macroscopic (or stoichiometric) binding constants have Arabic subscripts. These are related to the microscopic binding constants through the equations

$$K_1 = K_I + K_{II}$$

$$K_1 \cdot K_2 = K_I \cdot K_{II,I} = K_{II} \cdot K_{I,II}.$$

Table 1. *Amino acid sequences of the cys-containing fragments*[a]

Fragment	Amino acid sequence	Net charge
CysF1	KSPEELKGIF$_{10}$EKYAAKEGDP$_{20}$NQLSKEELKL$_{30}$LLQTEFPSCL$_{40}$KGM	−1
CysF2	STLDELF$_{50}$EELDKNGDGE$_{60}$VSFEEFQVLV$_{70}$KKCSQ	−6

[a] Calcium ligand coordinates in the intact protein are indicated with bold characters.

The cooperativity of calcium binding is defined in terms of $\Delta\Delta G$:

$$\Delta\Delta G \equiv -RT\ln(K_{1,II}/K_1) = -RT\ln(K_{II,1}/K_{II}).$$

$-\Delta\Delta G$ is positive for positive cooperativity ($K_{1,II} > K_1$) and can be rewritten as

$$-\Delta\Delta G = RT\ln(4K_2/K_1) + RT\ln[(\eta + 1)^2/4\eta],$$

where $\eta = K_{II}/K_1$. A lower limit to $-\Delta\Delta G$ can be calculated from the macroscopic binding constants as

$$-\Delta\Delta G_{\eta=1} = RT\ln(4K_2/K_1).$$

Results

Production of CNBr fragments of (L39C + P43M + I73C): Proof of SS-bond

The cysteine-free fragments F1 and F2 are readily produced by CNBr cleavage at the Met 43–Ser-44 peptide bond (and the Met 0–Lys 1 bond) of the calbindin D_{9k} mutant P43M, followed by separation on an ion exchange column (DEAE-Sephacel) using a NaCl gradient (Finn et al., 1992). Agarose gel electrophoresis in the presence of EDTA of the cleaved P43M yields two bands corresponding to F1 and F2. CNBr cleavage of (L39C + P43M + I73C) was followed by attempts to separate cysF1 and cysF2 by ion exchange chromatography and agarose gel electrophoresis using exactly the same buffers and gradient as for P43M. Separation of cysF1 and cysF2 under these conditions was found to be completely impossible. However, when a large excess of disulfide reducing agent (10 mM DTT) was added to the cleaved (L39C + P43M + I73C) as well as to the elution buffers, cysF2 and cysF1 could be isolated from each other on an ion-exchange column. When a large excess of DTT is added, the cleaved (L39C + P43M + I73C) also separates on agarose gel electrophoresis in the presence of EDTA into two bands corresponding to cysF1 and cysF2 (Fig. 3A). These results imply that the two cysteines in (L39C + P43M + I73C) form an SS-bond spontaneously under air oxidation.

In the presence of 10 mM DTT, cysF1 and cysF2 have the same mobilities as their cysteine-free counterparts on agarose gel electrophoresis in 2 mM EDTA, which separates mainly according to difference in total charge. In the absence of reducing agent the mobility towards the positive pole is significantly increased for cysF2 (cf. Fig. 3B). The net charge of cysF2 is −6 for a monomer and −12 for a dimer (in the absence of calcium).

Kinetics of heterodimer formation

The kinetics of heterodimer formation was followed by agarose gel electrophoresis at different times after mixing two homodimers in equimolar amounts, either $(F1)_2$ with $(F2)_2$, $(cysF1)_2$ with $(cysF2)_2$, $(cysF1)_2$ with $(F2)_2$, or $(F1)_2$ with $(cysF2)_2$.

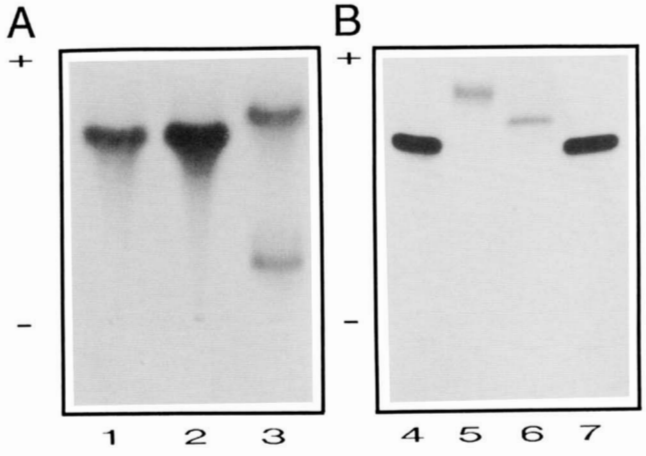

Fig. 3. Agarose gel electrophoresis in the presence of 2 mM EDTA. **A:** Lane 1, P43M; 2, (L39C + P43M + I73C) after CNBr cleavage of the 43–44 peptide bond; 3, same as lane 2 but with a large excess of DTT. **B:** Lane 4, P43M; 5, cysF2; 6, cysF2 with a large excess of DTT; 7, P43M.

When the cysteine-free homodimers, $(F1)_2$ and $(F2)_2$, are mixed with each other in the presence of calcium, formation of F1 + F2 heterodimer is a rapid process and goes to completion within the dead time (a minute), i.e., the time it takes to apply the sample and start the electrophoresis. However, when either one or both homodimers contain cysteine residues, the reaction is significantly retarded and is half complete in 30–60 min (with protein concentrations near 1 mM). At equilibrium all material is converted to heterodimers that have similar (but not identical) mobility on agarose gel as the F1 + F2 heterodimer. This is exemplified in Figure 4 for the case of $(cysF1)_2$ reacting with $(F2)_2$. In a control experiment $(cysF1)_2$ and $(cysF2)_2$ were mixed in the presence of 10 mM DTT. In this case heterodimer formation was complete within the dead time (a minute). The only straightforward interpretation of the lower reaction rate observed for cysteine-containing homodimers is that in each of $(cysF1)_2$ and $(cysF2)_2$ the two (identical) monomers are linked by disulfide bonds.

The same set of experiments was carried out also in the absence of calcium. When one or both fragments lack cysteines it is not possible to detect heterodimers on agarose gel electrophoresis in the presence of EDTA, even several days after mixing. Mixing of $(cysF1)_2$ with $(cysF2)_2$, however, results in stoichiometric formation of heterodimer. The reaction rate is in this case similar to that observed in the presence of calcium.

Relative stabilities of hetero- and homodimers

The kinetic experiments of heterodimer formation from one cysteine-free and one cysteine-containing homodimer

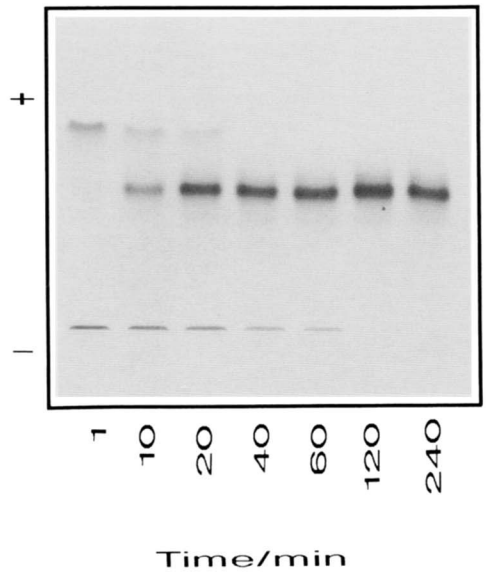

Fig. 4. Kinetics of heterodimer formation in the presence of calcium. Agarose gel electrophoresis run at different times (minutes) after mixing $(cysF1)_2$ and $(F2)_2$. The middle band corresponds to a heterodimer of cysF1 and F2 and the band closest to the positive pole to F2. $(CysF1)_2$ has very low net charge and has just barely entered the gel. Both $(F2)_2$ and $(cysF1)_2$ are colored more weakly than the heterodimer (Coomassie blue staining).

also provide information on the relative stabilities of the different species. In the presence of calcium the heterodimer is much more stable than any of the homodimers and the difference in stability is so large that it cannot be compensated for by SS-bond formation within the homodimers. In contrast, the experiments performed in the absence of calcium show that the heterodimer is still more favorable than each homodimer, but in this case the difference is small enough to be overcome by SS-bond formation in any of the homodimers.

Calcium binding to (L39C + P43M + I73C) and P43M

The macroscopic calcium binding constants, K_1 and K_2, were determined for P43M and (L39C + P43M + I73C) from Ca^{2+} titrations in the presence of the chromophoric chelator quin 2, as exemplified in Figure 5A. The results obtained at high (2 mM Tris + 0.15 M KCl) and low (2 mM Tris) ionic strength are summarized in Table 2. The total free energy change on binding two calcium ions is calculated as $\Delta G_{tot} = -RT \ln(K_1 K_2)$ and a lower limit to $-\Delta\Delta G$, the free energy of interaction between the sites, as $-\Delta\Delta G_{\eta=1} = RT \ln(4K_2/K_1)$. The values of $-\Delta\Delta G_{\eta=1}$ obtained at low ionic strength in five individual titrations on each of P43M and (L39C + P43M + I73C) are shown with filled symbols in Figure 5C. The values of $-\Delta\Delta G_{\eta=1}$ that give twice the χ^2 of the optimal fit are indicated. The analysis of these limits is described in the methods section and illustrated in Figure 5B. The average values

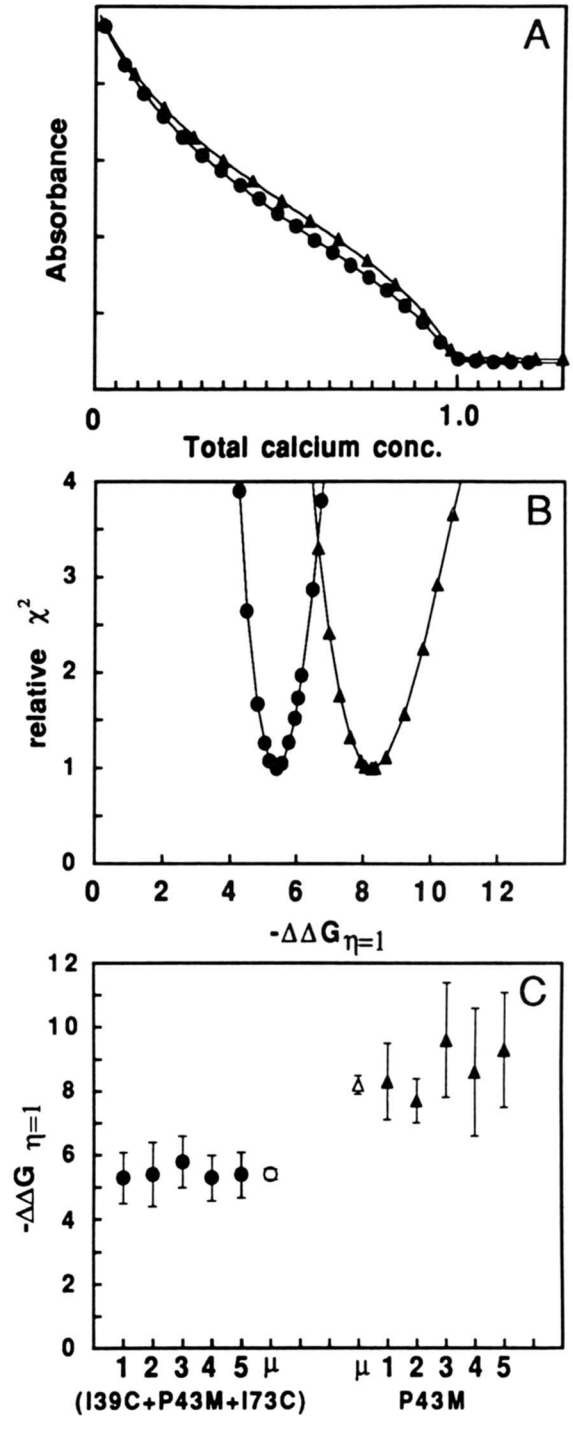

Fig. 5. A: Ca^{2+} titrations of in the presence of quin 2: absorbance at 263 nm (normalized) versus total calcium concentration (normalized). Experimental points for (L39C + P43M + I73C) (●) and for P43M (▲). Calculated curves (——) of optimal fit to the data points. **B:** Relative χ^2 for a series of fits to the data points in A using different fixed values of $-\Delta\Delta G_{\eta=1}$: (L39C + P43M + I73C) (●) and P43M (▲). **C:** Results from five individual titrations of (L39C + P43M + I73C) (●) and five of P43M (▲). The horizontal bars for each individual titration are set to include the values of $-\Delta\Delta G_{\eta=1}$ giving twice the χ^2 of the best fit. Note that these values are proportional to (and in general larger than) the standard deviation. The averages of five titrations are shown with open symbols together with error bars indicating the standard deviations of the averages.

(cf. Table 2) of the five titrations in each case are displayed with open symbols in Figure 5C, with vertical bars corresponding to $\pm\sigma$ (σ = standard deviation). The total calcium affinity is thus hardly affected by the disulfide bond, whereas the value of $-\Delta\Delta G_{\eta=1}$ is lowered. The value of $-\Delta\Delta G_{\eta=1}$ is lower for (L39C + P43M + I73C) than for P43M also at 0.15 M KCl.

The total free energy change on binding two calcium ions, ΔG_{tot}, is determined with high precision in the chelator experiments. The value of $-\Delta\Delta G_{\eta=1}$ is calculated from the ratio of the two macroscopic binding constants and is therefore critically dependent on precise measurements of both binding constants. The present achievement of good precision also in the values of $-\Delta\Delta G_{\eta=1}$ relies on low initial calcium concentrations and accurate determination thereof, as well as the mode of data analysis. Systematic errors introduced from deviations in endpoint values are avoided by fitting directly to the measured quantity, i.e., absorbance versus total calcium concentration. All data points thus contribute to determination of the absorbances in calcium-free and calcium-loaded solution, as well as the protein concentration. The distribution of the total binding affinity (K_1K_2) into the individual macroscopic binding constants is therefore obtained with good precision.

The ratio of the affinities for the two Ca^{2+} sites, $\eta = K_{II}/K_I$, was determined from Ca^{2+} titrations followed by ^1H NMR as outlined in detail elsewhere (Linse et al., 1991). The values of η that give the best fits to these titrations are 1.7 for P43M and 1.8 for (L39C + P43M + I73C). The (asymmetric) uncertainty range for η is 1.0–2.5 in both cases, which means that $RT\ln[(\eta+1)/4\eta] = 0.3 \pm 0.3$. Adding this to the 95% confidence intervals for $-\Delta\Delta G_{\eta=1}$, $-\Delta\Delta G$ can be estimated as 8.5 ± 1.1 kJ·mol^{-1} for P43M and 5.7 ± 0.6 kJ·mol^{-1} for (L39C + P43M + I73C). A $-\Delta\Delta G$ value of 8.5 kJ·mol^{-1} means that binding of calcium to one of the sites leads to a 31-fold increase in the affinity for the other site (i.e., $K_{I,II}/K_I = 31$), whereas 5.7 kJ·mol^{-1} corresponds to a 10-fold increase.

Calcium binding to homodimers

The two macroscopic binding constants of each of $(cysF1)_2$ and $(cysF2)_2$ were assessed with two different techniques to monitor calcium binding: (1) the CD method, which measures ellipticity changes in the homodimer, and (2) the chelator method, which utilizes a chromophoric chelator, 5,5′-Br_2-BAPTA, the absorbance of which changes on calcium binding. One titration of $(cysF2)_2$ using the chelator method is shown in Figure 6A, and one titration of $(cysF1)_2$ using the CD method is shown in Figure 6C. Both types of experiments unambiguously show that two Ca^{2+} ions are bound per homodimer. The measured number of calcium ions bound per dimer is 2.06 ± 0.13 for $(cysF1)_2$ and 1.99 ± 0.15 for $(cysF2)_2$, as averaged over all titrations with both methods. The CD and chelator methods were found to give similar values of the product of K_1 and K_2. The values reported for each homodimer in Table 2 are therefore averaged over all titrations with both methods at low and high ionic strength, respectively. At low ionic strength both homodimers bind calcium with roughly the same affinity ($\sqrt{K_1K_2} = 10^6$ M^{-1}). The salt dependence of ΔG_{tot} is stronger for $(cysF2)_2$ than for $(cysF1)_2$, but much weaker than for the intact protein. The decrease in $-\Delta G_{tot}$ when going from low (2 mM Tris) to high (2 mM Tris + 0.15 M KCl) ionic strength is 22 kJ·mol^{-1} for the intact protein, but only 6 and 11 kJ·mol^{-1} for $(cysF1)_2$ and $(cysF2)_2$, respectively.

Attempts to fit the titration data obtained in the presence of chelator without allowing for positive cooperativity led in each individual titration to a 5–25-fold increase in χ^2 as compared to the best fit obtained with positive cooperativity. The dependence of χ^2 on $-\Delta\Delta G$ (Fig. 6B) is, however, much weaker than for the heterodimers (Fig. 5B).

Kinetics of calcium binding

Calcium binding to each homodimer was also followed by ^1H NMR. Again it was found that two calcium ions

Table 2. *Macroscopic calcium binding constants*

Protein	[KCl] (M)	log K_1	log K_2	$-\Delta G_{tot}$ (kJ·mol^{-1})	$-\Delta\Delta G_{\eta=1}$ (kJ·mol^{-1})	N
P43M	–	7.75 ± 0.04	8.59 ± 0.04	93.3 ± 0.1	8.2 ± 0.3	5
(L39C + P43M + I73C)	–	7.92 ± 0.02	8.26 ± 0.02	92.4 ± 0.1	5.4 ± 0.1	5
P43M	0.15	5.98 ± 0.06	6.50 ± 0.06	71.4 ± 0.2	6.4 ± 1.0	5
(L39C + P43M + I73C)	0.15	6.06 ± 0.02	6.23 ± 0.02	70.3 ± 0.2	4.4 ± 0.1	5
$(CysF1)_2$	–			68.5 ± 0.9		4
$(CysF1)_2$	0.15			62.2 ± 0.9		2
$(CysF2)_2$	–			68.5 ± 0.9		4
$(CysF2)_2$	0.15			57.7 ± 0.9		3

[a] log K_1, ^{10}log K_1; log K_2, ^{10}log K_2; ΔG_{tot}, $-RT\ln(K_1K_2)$; $-\Delta\Delta G_{\eta=1}$, $RT\ln(4K_2/K_1)$; N, number of experiments. The standard deviations are given as $\pm\sigma$. The 95% confidence interval with five experiments is $\pm 2.8\sigma$. The data were collected in 2 mM Tris plus 0.15 M KCl or no added salt (–).

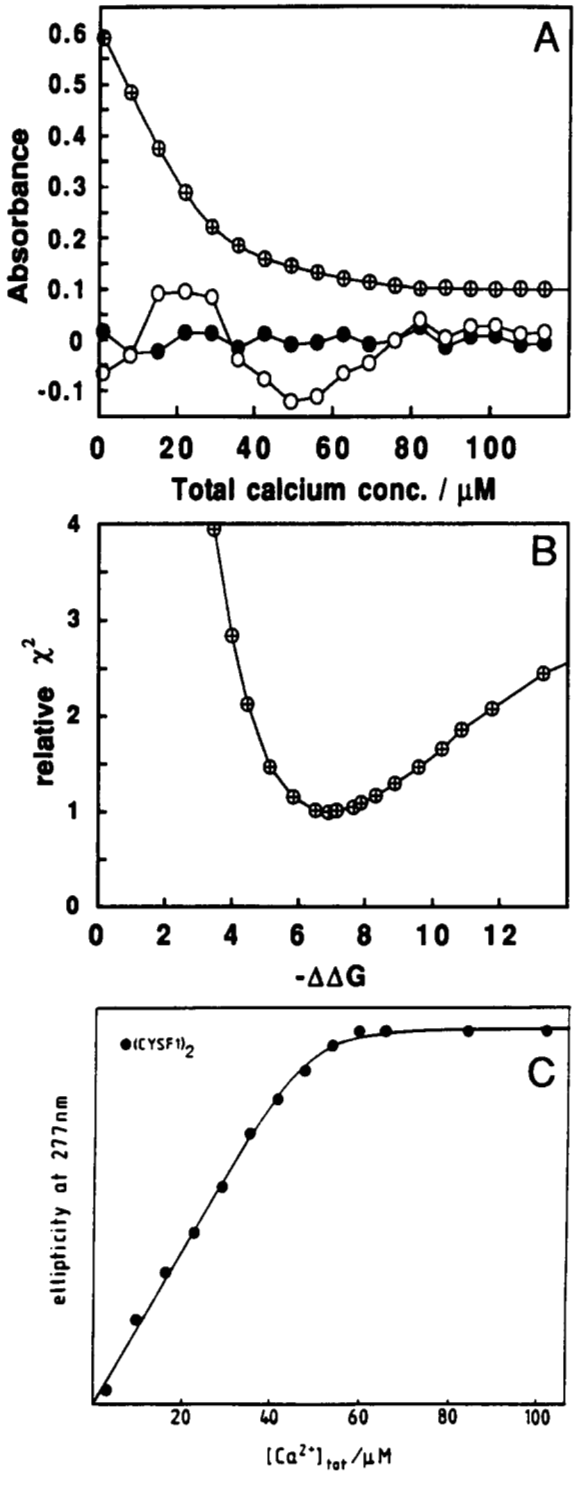

Fig. 6. A: Ca^{2+} titration of 21.8 μM $(cysF2)_2$ in the presence of 31.0 μM 5,5′-Br_2-BAPTA: experimental points (⊕), calculated curve that gives optimal fit to the experimental points (——), and 10× residuals for this fit (●). Residuals (10×) for the best fit obtained without allowing for cooperativity (○). **B:** Relative χ^2 for a series of fits to the data points in A using different fixed values of $-\Delta\Delta G$. **C:** Ca^{2+} titration of $(cysF1)_2$ as followed by CD: ellipticity at 277.5 nm versus total calcium concentration. Experimental points (●) and calculated curve of optima fit to the data points (——). The protein concentration was 24.1 μM dimer before the Ca^{2+} additions. The total dilution at the last titration point shown was 9.3%.

were bound to each homodimer. In addition, these measurements provide information on the kinetics of calcium binding. On the ^1H NMR time scale, Ca^{2+} ions bound to $(cysF1)_2$ are in slow exchange with Ca^{2+} ions in the bulk solution. Some proton NMR signals decrease in intensity and new ones appear and increase in intensity as calcium is gradually added. The process continues up to two calcium ions per dimer, and after that no further changes to the spectrum are observed. The off-rate for calcium is thus $\leq 10\ s^{-1}$. For $(cysF2)_2$ all ^1H NMR resonances are substantially broadened and some lines shift when calcium is added. Maximal broadening is observed at $c:a$ one calcium per dimer. At higher calcium additions the signals become sharper again and at two calcium ions per dimer the linewidth is roughly the same as in the absence of calcium. No further changes of the spectrum are observed at calcium additions above two calcium per dimer. The calcium off-rate for $(cysF2)_2$ is estimated from the maximal linewidth as 100–200 s^{-1}. The general patterns observed in the ^1H NMR titrations of both homodimers are thus the same as reported for their cysteine-free counterparts (Finn et al., 1992). Because both homodimers bind calcium with roughly the same affinity, it appears that the calcium on-rate for $(cysF2)_2$ exceeds that of $(cysF1)_2$ by a factor of 10 or more.

Stability of heterodimers

The calcium form of calbindin D_{9k} is too stable to be denatured by 10 M urea or at temperatures below 110 °C. The present experiments are therefore limited to the Ca^{2+}-free forms. Urea denaturation profiles of the Ca-free forms of (L39C + P43M + I73C), the cysF1 + cysF2 heterodimer, P43M, and the F1 + F2 heterodimer are shown in Figure 7A. The values of C_m, the urea concentration at half denaturation, as deduced from these profiles can be found in Table 3. If we compare the values of C_m for the F1 + F2 heterodimer (no covalent linkage; $C_m \approx 1$ M), P43M (one covalent linkage; $C_m = 5.3$ M), the cysF1 + cysF2 heterodimer (one covalent linkage; $C_m = 5.3$ M), and (L39C + P43M + I73C) (two covalent linkages; $C_m = 8.0$ M) it appears that the stability is the same for both types of heterodimer with one covalent bond.

The data points in the transition zone have been used to calculate the free energy of unfolding as $\Delta G_U = -RT \ln[(1-\theta)/\theta]$, where the normalized ellipticity, θ, is the fraction of native protein and $(1-\theta)$ is the fraction of unfolded protein (Fig. 7C). Because the dependence of ΔG_U on the urea concentration is nearly linear for (L39C + P43M + I73C) but appears to be nonlinear for P43M, extrapolation to 0 M urea would be very uncertain (see Wendt et al., 1988), and it is safer to make a comparison at 6.7 M urea. At this urea concentration, apo (L39C + P43M + I73C) is 8 $kJ \cdot mol^{-1}$ more stable than apo P43M.

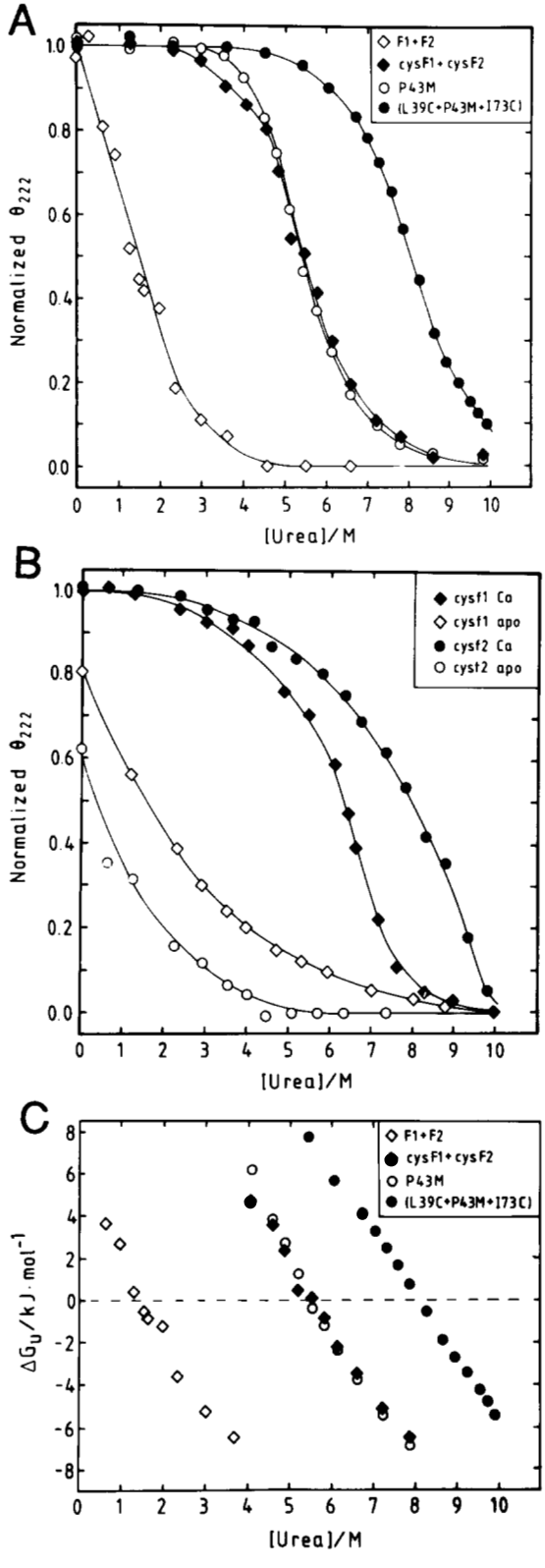

Fig. 7. Urea denaturation profiles. Normalized ellipticity at 222 nm as a function of urea concentration. **A:** F1 + F2 heterodimer (◇), cysF1 + cysF2 heterodimer (◆), P43M (○), and (L39C + P43M + I73C) (●). **B:** $(CysF1)_2 \cdot Ca_2$ (◆), $(cysF1)_2$ apo (◇), $(cysF2)_2Ca_2$ (●), and $(cysF2)_2$ apo (○). **C:** Free energy of unfolding, ΔG_U, as calculated from the data in A. F1 + F2 heterodimer (◇), cysF1 + cysF2 heterodimer (◆), P43M (○), and (L39C + P43M + I73C) (●).

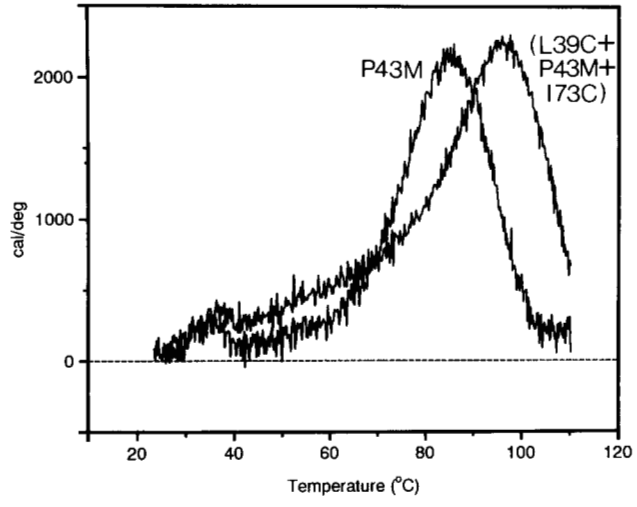

Fig. 8. Results from differential scanning calorimetry of calcium-free P43M and (L39C + P43M + I73C).

The thermal stability of the calcium-free P43M is very high (and the same as for the wild type) and has increased by 10 °C in the mutant (L39C + P43M + I73C). The melting curves as measured with differential scanning calorimetry are shown in Figure 8. The values of T_m, the transition midpoint, are summarized in Table 3.

Stability of the homodimers

Urea denaturation profiles of $(cysF1)_2$ and $(cysF2)_2$ in the presence of either EDTA or Ca^{2+} are shown in Figure 7B. In this figure the ellipticity of both the calcium and apo forms is normalized against that of the calcium form with an ellipticity of 1.0 corresponding to 100% native calcium form. The values of C_m, the urea concentration at half denaturation, as deduced from these profiles can be found in Table 3. The thermal stabilities of the cal-

Table 3. *Stability parameters*

Protein	Form	T_m/ °C	C_m/M
P43M	apo	85±	5.3
(L39C + P43M + I73C)	apo	≥95	8.0
cysF1 + cysF2 heterodimer	apo		5.3
F1 + F2 heterodimer	apo		1.5
$(CysF1)_2$	Ca	93 ± 2	6.2
$(CysF1)_2$	apo		2.2
$(F1)_2$	Ca	80 ± 4	≈3[b]
$(CysF2)_2$	Ca	91 ± 2	7.5
$(CysF2)_2$	apo		1.0
$(F2)_2$	Ca	59 ± 2	≈1.5[b]

[a] T_m is the transition midpoint of thermal denaturation and C_m is the urea concentration of half denaturation.
[b] Data from M. Akke (pers. comm.).

cium forms of the homodimers were assessed by differential scanning calorimetry. For comparison the thermal stabilities of the cysteine-free homodimers were also determined in the presence of calcium. The melting process as measured with differential scanning calorimetry appears to be complex and has been interpreted only in terms of the transition midpoint, T_m. The values of T_m are given in Table 3.

The enormous increase in C_m as observed in the presence of calcium, from ≈1.5 M urea for $(F2)_2$ to 7.5 M urea for $(cysF2)_2$, is paralleled by a large increase in T_m, from 59 to 91 °C. The observed increases in C_m and T_m when going from $(F1)_2$ to $(cysF1)_2$ (Ca-forms) are both somewhat smaller; from ≈3 to 6.2 M urea and from 80 to 93 °C.

Removal of calcium leads to a substantial destabilization of both $(cysF1)_2$ and $(cysF2)_2$, and it is evident from Figure 7B that the cysF2 homodimer is most sensitive to calcium removal. In the absence of urea, the ellipticity observed for apo $(cysF2)_2$ at 222 nm is only 60% of that in the calcium form. In addition the ^{1}H NMR spectrum of apo $(cysF2)_2$ consists of narrow lines with little shift dispersion. Thus, the cysF2 homodimer appears to loose a substantial degree of structure when calcium is released. $(cysF1)_2$, on the other hand appears to retain a higher degree of ordered structure in the apo state; the ellipticity at 222 nm is nearly 85% of that in the calcium form, and the ^{1}H NMR spectrum contains broader lines with significant shift dispersion.

^{113}Cd NMR

(L39C + P43M + I73C) was titrated with $^{113}Cd(NO_3)_2$. For additions up to 1 equivalent of cadmium a sharp resonance for $^{113}Cd^{2+}$ bound to site II appears at −99.9 ppm. The intensity of this signal increases linearly up to a Cd^{2+}:protein ratio of 1. At higher $^{113}Cd^{2+}$ concentrations this resonance is displaced towards lower frequency as a result of Cd^{2+} entering into site I. The site II resonance is also broadened between 1 and 2 equivalents of Cd^{2+}. At Cd^{2+}:protein ratios exceeding 2 it has moved to −106 ppm and become sharp. The resonance from $^{113}Cd^{2+}$ ions bound to site I is broad and appears at −144 ± 10 ppm. All features of the Cd^{2+}-titration of (L39C + P43M + I73C) as followed by $^{113}Cd^{2+}$ NMR are thus closely similar to those of the wild-type protein (Linse et al., 1987).

^{1}H NMR assignments of (L39C + P43M + I73C)

The differences in backbone chemical shifts between the calcium forms of P43M and (L39C + P43M + I73C) are so small that most of the NH–C$^\alpha$H resonances of (L39C + P43M + I73C) could be preliminarily assigned by comparing the COSY, R-COSY, and TOCSY spectra of the two proteins. These preliminary assignments were then confirmed by NH–NH and NH–C$^\alpha$H crosspeaks in the 200 ms NOESY spectrum, which also led to identification of the majority of the remaining NH–C$^\alpha$H resonances. Resonances from the following residues could not be assigned by this simple approach: G18, D19, K41, G42, M43, S44, and all proline residues. D58 and K72 have C$^\alpha$H shifts close to the water resonance at 37 °C and the C$^\alpha$H shifts are therefore set to 4.65. Structural shifts (i.e., chemical shifts minus random coil shifts [Wüthrich, 1986]) of backbone protons in the Ca_2 form of (L39C + P43M + I73C) are shown in Figure 9 in comparison with P43M (Johansson et al., 1993). On comparing the two proteins it appears that the disulfide bridge is well accommodated and the only region where minor conformational changes cannot be excluded is in the close vicinity of the SS-bond itself. It is not possible to say whether the small chemical shift effects (≤0.3 ppm) observed for residues 38, 39, and 70–73 are the result of a minor rearrangement or represent a more direct effect of the amino acid substitutions.

^{1}H NMR assignments of $(cysF2)_2 \cdot Ca_2$

The proton NMR spectrum of calcium-loaded $(cysF2)_2$ clearly shows that the dimer is symmetric since only one spin-system could be identified for each residue in the monomer. Many of the 33 residues have NH and C$^\alpha$H shifts that are very similar to the shifts in intact calcium-loaded calbindin D_{9k}. A majority of the NH–C$^\alpha$H crosspeaks in the COSY spectrum could thus be identified by comparison with the shifts in P43M (Johansson et al., 1993). These preliminary assignments were then confirmed by NH–NH and NH–C$^\alpha$H crosspeaks in the 200-ms NOESY spectrum, which also led to identification of all NH and/or C$^\alpha$H resonances except for S44, T45, E51, and E52. One remaining NH–C$^\alpha$H crosspeak could be assigned to either E51 or E52 based on a NOE connectivity from the C$^\alpha$H to the NH of L53.

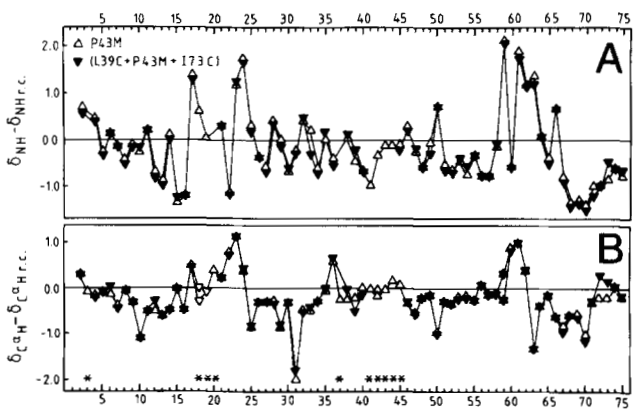

Fig. 9. Chemical shift minus random coil shift (ppm units) for backbone protons in (L39C + P43M + I73C) (▼) and P43M (△). **A:** NH. **B:** C$^\alpha$H.

Side-chain resonances were assigned using R-COSY in H_2O and COSY and R-COSY in D_2O. Three extra spin-systems were identified in the latter two spectra. The chemical shift patterns of serine, threonine and glutamic acid are very different (Wüthrich, 1986). The chemical shifts of of S44, T45, and the remaining of E51 and E52 could thus be assigned. Because there is no clear distinction between E51 and E52, the two sets of signals that are found to arise from either E51 or E52 are labeled E51/52 in the assignment list provided as Supplementary material on the Diskette Appendix.

Structural shifts of backbone protons are shown in Figure 10A and B in comparison with the structural shifts of the corresponding residues in intact, calcium-loaded P43M (Johansson et al., 1993). In this figure the NH shift of E51 or E52 is plotted for both residues and the distinction between the $C^{\alpha}H$ shifts of E51 and E52 is of course arbitrary. The observed differences are surprisingly small and involve mainly residues number 50, 56, 61–63, and 69–75, of which 56 and 61–63 are in the calcium-binding loop (cf. Table 1). Wishart et al. (1992) have suggested that continuous stretches of structural $C^{\alpha}H$ shifts above 0.1 ppm and below −0.1 ppm are indicative of β-sheet and α-helix conformation, respectively. Such an analysis would indicate that residue segments 44–70 and 74–75 in $(cysF2)_2$ adopt the same secondary structure as the corresponding segments in P43M. The method of Wishart et al. (1992) cannot handle residues 71–73 for which the structural $C^{\alpha}H$ shifts are small in P43M and small absolute changes lead to structural $C^{\alpha}H$ shifts above −0.1 ppm.

The scalar $^3J_{HH}$ NH-$C^{\alpha}H$ coupling constants of $(cysF2)_2$ and P43M are also very similar, as shown in Figure 10C. These coupling constants are dependent on the local conformation of the backbone, and the comparison in Figure 10C can be taken as additional support of very similar secondary structures in $(cysF2)_2$ and P43M. In fact, no difference was observed for residues 72 and 73. Together, the chemical shift and coupling constant analyses suggest that the backbone fold of each monomer in $(cysF2)_2$ is the same as for residues 44–75 in P43M. An NOE between Asp 54 NH and Val 61 $C^{\gamma}H$ shows that the two ends of the loop in each monomer are in close proximity.

Side-chain chemical shifts are compared in Figure 11. Since no stereospecific assignments are made in the present work, we have chosen to present the smallest possible shift differences for each side chain when comparing $(cysF2)_2$ and P43M. All observed effects are thus real. Large effects (>0.2 ppm) are observed for L46$C^{\beta}H$, L49$C^{\beta}H$, F50$C^{\delta}H$, E60$C^{\beta}H$, V61$C^{\gamma}H$, F66$C^{\delta}H$, F66$C^{\epsilon}H$, and V70$C^{\gamma}H$, all of which interact in P43M with residues in the N-terminal EF-hand – interactions that can of course not take place in $(cysF2)_2$.

With the knowledge that the general fold of each cysF2 monomer is highly similar to the fold of the corresponding residues in P43M (cf. above), several observed NOEs that involve F50 can be judged as highly unlikely to be intramonomeric, because the corresponding protons are significantly more than 5 Å apart in intact calbindin D_{9k}. A few of these presumably intermonomeric NOEs are listed in Table 4. Some NOEs involving residues 59–64 suggest the existence of an antiparallel β-sheet between the loops of cysF2 and cysF2′, as depicted in Figure 12. Primed and unprimed notation is used to distinguish the two monomers. One characteristic NOE is necessarily missing since V61NH and V61′NH are identical. Additional support of a β-sheet comes from slow exchange with solvent water

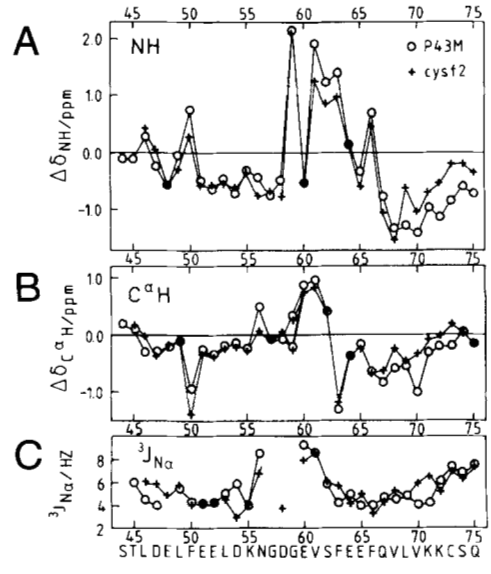

Fig. 10. Chemical shift minus random coil shift for backbone protons in the calcium loaded forms of the cysF2 homodimer (+) and P43M (O). **A:** NH. **B:** $C^{\alpha}H$. **C:** ^3J NH-$C^{\alpha}H$ coupling constants.

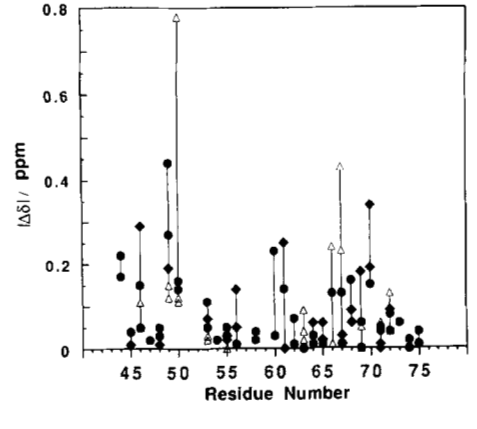

Fig. 11. Comparison of side-chain chemical shifts. Absolute value of chemical shift difference between $(cysF2)_2$ and P43M. $C^{\beta}H$ (●); $C^{\gamma}H$ (◆); $C^{\delta}H$, $C^{\epsilon}H$, $C^{\zeta}H$, and NH_2 (△). Vertical lines connect points for the same residue.

Table 4. *Some observed NOEs[a] that are likely to be intermonomeric*

NOE	Distance in intact calbindin[b] (Å)
F50NH-F66C$^{\delta}$H	9.8, 11.5
F50C$^{\alpha}$H-F66C$^{\epsilon}$H	10.1, 12.2
F50C$^{\beta}$H-F63C$^{\delta}$H	15.3, 17.2
F50C$^{\beta}$H-F66C$^{\delta}$H	10.4, 12.7
F50C$^{\beta}$H-F66C$^{\epsilon}$H	10.7, 13.0
F50C$^{\beta}$H-Q67C$^{\gamma}$H	16.4
F50C$^{\delta}$H-F66C$^{\beta}$H	9.7, 11.6
F50C$^{\delta}$H-F63C$^{\epsilon}$H	14.1, 15.9, 16.1, 17.8
F50C$^{\epsilon}$H-F66C$^{\beta}$H	9.4, 11.3
F50C$^{\epsilon}$H-F63C$^{\beta}$H	12.6, 14.3
F50C$^{\epsilon}$H-Q67C$^{\gamma}$H	14.8, 16.5
F50C$^{\epsilon}$H-F63NH	10.5, 12.0

[a] NOEs observed in 200-ms NOESY in H_2O.
[b] Carbon-carbon distances in the crystal structure of calbindin D_{9k} (Szebenyi & Moffat, 1986). Because no stereospecific assignments are made, all distances are given when there is more than one option.

as observed for the NH of Val 61 in a one-dimensional exchange-out experiment ($k_{ex} \approx 10^{-4}$ s^{-1} at pH 6.0). If we take two cysF2 monomers (with the same conformation as for the corresponding residues in P43M), rotate one of them 180° and position them with the hydrophobic sides against each other and the suggested β-strands in an antiparallel arrangement, then Phe 50 of one monomer will come close to Phe 63′ and Phe 66′ of the other monomer. Interaction between F50, F63′, and F66′ would explain the NOEs listed in Table 4, and also the large shift changes observed for the side chains of F50 and L49.

The information from assignment, coupling constants and NOEs, together with the knowledge that the two cysteines form a disulfide bond, allows us to make a schematic sketch of the overall topology of the calcium form of the cysF2 homodimer (Fig. 13).

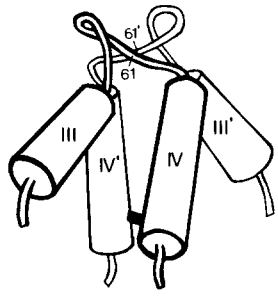

Fig. 13. Schematic drawing of the topology of $(cysF2)_2$.

CD spectra

Near-UV CD spectra of (L39C + P43M + I73C) and P43M, in the absence and presence of calcium, are shown in Figure 14. In both proteins Tyr 13 gives a high, but Ca^{2+}-dependent, ellipticity around 277 nm, in the same manner as reported for porcine calbindin D_{9k} (Dorrington et al., 1978). For both mutants there is a similar difference in ellipticity between the apo and calcium forms. Both in the absence and presence of calcium the ellipticity is lower for (L39C + P43M + I73C) than for P43M. The difference spectra between the two proteins have been calculated for both apo and calcium-loaded proteins (Fig. 14C). SS-bonds are known to give CD-signals in the near-UV range and the wavelength, intensity, and the sign of the ellipticity are all dependent on the conformation and rigidity of the SS-bond (Kahn, 1979).

Discussion

Proof of SS-bonds

Strong quantitative evidence of spontaneous SS-bond formation in (L39C + P43M + I73C) is given by the impossibility of separating its CNBr fragments at any detectable

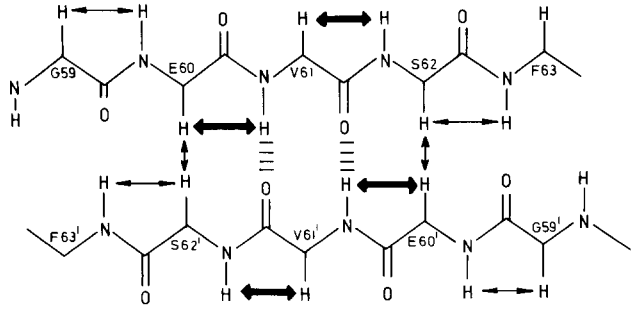

Fig. 12. NOEs observed in the β-sheet region of the calcium-loaded $(cysF2)_2$. Thicker arrows represent the strongest NOEs. The two hydrogen bonds that can be assigned on the basis of the NMR evidence are shown by cross-hatched vertical bars.

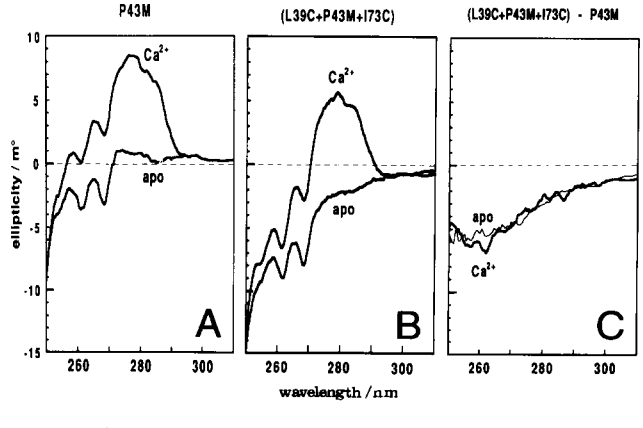

Fig. 14. Circular dichroism spectra of P43M (**A**) and (L39C + P43M + I73C) (**B**). These spectra were recorded for *c*:*a* of 200 μM protein in a 10-mm cuvette in the presence of excess calcium or excess EDTA. **C**: Difference spectra (between the two proteins).

level unless a large excess of DTT is added. The analysis of backbone ^{1}H NMR shifts shows that the disulfide bond is well accommodated in the calbindin D_{9k} fold with at most minor alteration of the local structure around the substitution sites. The ^{113}Cd NMR studies show that the disulfide does not interfere directly with the metal-ion binding sites.

The results of the kinetic studies of heterodimer formation show that $(cysF1)_2$ and $(cysF2)_2$ each contain disulfide bonds between the two identical monomers. This type of experiment cannot rule out the possibility that a small fraction of the homodimers lack disulfide. In the case of calcium free $(cysF2)_2$ agarose gel electrophoresis in the absence and presence of DTT (Fig. 3B) shows that at least 95% of the dimers are disulfide linked. The much lower net charge on cysF1 makes it difficult to discriminate between monomers and dimers on agarose gels. The large stabilization achieved by crosslinking in each homodimer means that urea denaturation profiles of a mixture of disulfide-linked and noncrosslinked dimers would show two transitions with amplitudes reflecting the relative populations. The quality of the present data allows us to say that more than 90% of $(cysF1)_2$ are disulfide linked.

Calcium binding to heterodimers

The results of the present study show that introduction of an SS-bond in calbindin D_{9k} partly reduces the cooperativity of calcium binding, but has only minor effects on the total affinity. This conclusion is based on combined results of two different titration techniques, one that measures the macroscopic Ca^{2+} binding constants and one that specifies the ratio of the affinities for the two Ca^{2+} sites. The Ca^{2+} titrations as followed by ^{1}H NMR show that the inserted disulfide has no measurable effect on the ratio of the affinities for the two Ca^{2+} sites. This finding is in good agreement with the results of the ^{113}Cd NMR, which indicate that the disulfide, which is located over 17 Å from the calcium sites, does not interfere with these sites. Thus, the reduction of $-\Delta\Delta G_{\eta=1}$, as observed in the chelator experiments, is caused by a reduced cooperativity in the disulfide mutant.

Reduction of the cooperativity could arise from changes in dynamics of one or more protein species (the zero-, one-, and/or two-calcium forms). High-resolution NMR studies by Akke et al. (1991) have shown that the binding of a metal ion to the C-terminal site reduces the flexibility of both EF-hands, including the helices. This was suggested to increase the calcium affinity of the other site, i.e., cooperativity (Akke et al., 1991). Cooper and Dryden (1984) pointed out that ligand-induced changes in protein dynamics can produce allosteric communication between distinct binding sites even in the absence of macromolecular conformational change. In addition, Rebek et al. (1985) proposed a model of cooperativity in small symmetric crown ethers that is based on a large reduction in flexibility of both sites after binding of the first metal ion. Mutations that increase the rigidity of the calcium-free state of calbindin D_{9k} might abolish this type of mechanism for cooperativity. Thus, future NMR studies of the dynamics of (L39C + P43M + I73C) with zero, one, and two metal ions bound would be of great value in understanding the observed reduction of cooperativity in this mutant. Qualitative NH-exchange studies indicate that the rates of fluctuations in calcium-free (L39C + P43M + I73C) are significantly lower than in the wild type (data not shown).

The cooperativity of calcium binding to calbindin D_{9k} is likely to rely on several different mechanisms, since much larger effects on the cooperativity have been observed in some charge substitution mutants, e.g., (E17Q + D19N) where $-\Delta\Delta G_{\eta=1}$ is as low as 1.7 kJ·mol^{-1} at low ionic strength (Linse et al., 1991).

The values we report here for ΔG_{tot} and $-\Delta\Delta G_{\eta=1}$ of P43M are both different from the values for the wild type (Linse et al., 1991). The value of $-\Delta G_{tot}$ is somewhat lower in P43M, whereas $-\Delta\Delta G_{\eta=1}$ appears to be slightly higher. The same effects of the Pro 43 → Met substitution have been observed in our laboratory for mutants that have been studied with both proline and methionine in position 43.

Calcium binding to homodimers

The results of the measurements presented here clearly show that each homodimer binds two calcium ions with high affinity, at both low and high ionic strength. In contrast, Shaw et al. (1990, 1991) found that a homodimer of a 34-residue peptide, comprising the site III EF-hand in troponin C, binds only one calcium ion per homodimer with high affinity and that a second calcium ion is bound with 1,000-fold lower affinity. This implies very strong negative cooperativity, since a homodimer is symmetric with identical Ca^{2+} sites. In the present work, however, it appears that each homodimer binds calcium with positive cooperativity at both high and low ionic strength. In this context, it is valuable to consider the calcium binding studies of two calbindin mutants with the wild-type helices but with both Ca^{2+} loops having identical sequence, that of either wild-type loop I or loop II (Brodin et al., 1990). Both these mutants were found to bind two calcium ions with high affinity, which shows that there is no requirement for the loops to be different to form a functional unit that binds two calcium ions with similar affinity.

The Ca^{2+} titration methods used here fail to determine precise values of individual binding constants, and it is therefore not possible to quantitate the cooperativity of calcium binding. With the CD technique one has to play with very small differences between binding curves for cooperative and noncooperative binding, as the Ca^{2+} affinities are close to 10^6 M^{-1}. The accuracy of the other

method is limited by the fact that the chelator binds calcium *c:a* 10-fold more strongly than the homodimers. It is, however, clear that all titrations with the chelator method are best fitted by theoretical curves calculated with positive cooperativity (cf. Fig. 6B). The cooperativity of calcium binding to the homodimers could be quantitated by repeating the measurements in the presence of a chelator with a calcium affinity in the range $5 \cdot 10^5$ to $1 \cdot 10^6\ M^{-1}$, instead of $1 \cdot 10^7\ M^{-1}$ as for 5,5′-Br_2-BAPTA.

Stability of the heterodimers

The stabilization achieved with an SS-bond in calbindin D_{9k} is substantial. In addition, it was found that the stability of the protein with one covalent linkage is the same whether the bond is joining residues 43 and 44 or 39 and 73. The stabilization relative to the F1 + F2 heterodimer probably represents the entropic gain of a crosslink. More exactly, the terms should differ by the difference in destabilization of the complex due to strain introduced by the disulfide and peptide bond, respectively.

Stability of the homodimers

The stability of the noncrosslinked homodimers is rather low even for the calcium-loaded forms. The stabilization achieved by introducing a covalent crosslink between the two monomers in a dimer is quite remarkable, especially for the dimer of the fragment comprising the C-terminal EF-hand of calbindin D_{9k}. The stabilities of the noncrosslinked homodimers are of course concentration dependent, but since the measurements on $(F1)_2$ and $(F2)_2$ are made at roughly the same concentration ($\approx$0.5 mM for thermal denaturation and $\approx$15 μM for urea denaturations), it appears that the stabilization achieved by forming an SS-bond is much higher in $(cysF2)_2$ than in $(cysF1)_2$.

Naively, one might argue that the entropic gain of a crosslink would be the same in both cases. However, if we wish to understand the observed differences in stabilizing power we have to consider the exact location of the SS-bond in each homodimer. Residue cys73 in cysF2 is located near the C-terminal end of helix IV, but within the helix. Thus in the cysF2 dimer the SS-bond forms a direct linkage between helices IV and IV′, and literally forces the two (identical) EF-hands into close interaction with each other. Residue cys39 in cysF1 is located outside of helix II, which ends at residue 36 in the intact protein. The disulfide bond in the cysF1 homodimer is thus not within the regular EF-hand motifs, and the two EF-hands are connected by a rather long and flexible link involving at least six residues (37, 38, 39, 39′, 38′, and 37′). Apparently, the disulfide in this flexible link is not as effective in stabilizing the homodimer as the much shorter and more rigid link in $(cysF2)_2$.

Relative stabilities of hetero- and homodimers

Discussion of the relative stabilities of hetero- and homodimers is simplified if we look at each EF-hand subdomain as a unit with two surfaces: one curved surface exposed to water and one flatter surface in contact with the other EF-hand in the pair. The flatter surface is predominantly hydrophobic. The disposition of its hydrophobic residues and of the charged residues at the rim of the flatter surface is well optimized for interaction with the other EF-hand in the presence of calcium. When isolated, each EF-hand will form homodimers to avoid exposure of the hydrophobic surface. However, because the disposition of hydrophobic and charged residues is not optimized for interaction with an identical EF-hand, this interaction is not nearly as strong as with the other EF-hand. The difference is too large to be compensated for by a covalent linkage in the homodimer. Using the same simplified picture of an EF-hand, the results obtained in the absence of calcium indicate that the flatter surface has becomes less selective. A calcium-free EF-hand can more easily adapt to different interaction partners. In the present case it has been possible to shift the equilibrium condition from a complex with the natural partner (the other EF-hand in the native protein) to a complex with an unnatural partner (an identical EF-hand) by allowing for covalent linkage of homodimers but not heterodimers. The lower selectivity is probably linked to the increased rate of conformational fluctuations in the apo state.

Materials and methods

Chemicals

Quin 2 was from Fluka, Switzerland; urea was from Aristar, BDH; and DTT was from Bio-Rad. All other chemicals were of the highest purity commercially available.

Proteins

(L39C + P43M + I73C) and P43M were expressed in *Escherichia coli* and purified as previously described (Johansson et al., 1990). The purity was checked by agarose gel electrophoresis in the presence of either excess Ca^{2+} or excess EDTA, by isoelectric focusing, by sodium dodecyl sulfate-polyacrylamide gel electrophoresis, and by ^1H NMR.

Fragments

The Met 43–Ser 44 peptide bond (and the Met 0–Lys 1 peptide bond) in (L39C + P43M + I73C) was cleaved by CNBr (1,000 mol per mol protein) in the presence of 80% TFA for 20 h at room temperature under N_2 gas (Finn et al., 1992). The TFA and CNBr were then evaporated and the protein was dissolved in a solution of 5 mM

EDTA and 10 mM DTT (for reduction of the disulfide bond). Tris (1 M) was added to get a final pH of 7.5. The two fragments, cysF1 and cysF2, comprising residues 1–43 and 44–75, respectively, were then separated on a DEAE-Sephacel column in 10 mM Tris/HCl, pH 7.5 with 1 mM EDTA and 10 mM DTT. Elution of the fragments (with a linear NaCl gradient, 0 to 0.3 M) was assayed by agarose gel electrophoresis in the presence of 2 mM EDTA. After freeze-drying (lyophilization) of each fragment, NaCl, Tris, EDTA, and DTT were removed by separation on a Sephadex G25 column (with saturated NaCl applied just before the sample) as verified by ^{1}H NMR.

Cysteine-free fragments, F1 and F2, were obtained by the same method from P43M (Finn et al., 1992), except that no DTT is needed.

The cysF1 + cysF2 heterodimer was prepared by adding together equimolar amounts of the two cysteine-containing fragments and allowing for disulfide rearrangement for 24 h. Agarose gel electrophoresis was used to confirm that none of the fragments was in excess over the other. The F1 + F2 heterodimer was prepared in the same way from F1 and F2.

Circular dichroism

CD spectra and intensities were measured on a JASCO-500 spectropolarimeter, in a water-jacketed cuvette at 25 °C.

NMR spectra

^{1}H NMR spectra were recorded on a GE Omega 500 spectrometer at 500.13 MHz. One-dimensional spectra were recorded at pH 6.0 and room temperature. Two-dimensional spectra (COSY, R-COSY, TOCSY [120 ms mixing time], and NOESY [200 ms mixing time]) were recorded in H_2O at pH 6.0 and 37 °C or 27 °C. The in-house program MAGNE was extensively used in the assignment procedures. Backbone NH-C$^\alpha$H coupling constants were calculated from COSY spectra zero filled to a final size of 1,024 × 4,096 points, using a line-shape fitting routine in the MAGNE program. ^{113}Cd NMR spectra were obtained on a home-built spectrometer using a solenoidal probe and an Oxford Instruments 6T magnet at 56.55 MHz at room temperature and pH 6.5.

Calcium titration followed by ^{1}H NMR

$(cysF1)_2$, $(cysF2)_2$, P43M, or (L39C + P43M + I73C) was dissolved in H_2O (with 10% D_2O for the lock signal) to a concentration of 2 mM. Calcium was added in steps of 0.15 mol Ca^{2+} per mol monomer for the homodimers or in steps of 0.15 mol Ca^{2+} per mol heterodimer, followed by acquisition of one-dimensional ^{1}H NMR spectra.

Ca^{2+} binding constants

The two macroscopic binding constants of hetero- or homodimer were determined in 2 mM Tris/HCl buffer at pH 7.5, room temperature. Measurements were performed at both high (0.15 M KCl) and low (no salt added) ionic strength.

Chelator method

Each protein was titrated with calcium in the presence of a chromophoric chelator: 5,5′-Br_2-BAPTA (for homodimers) or quin 2 (for heterodimers), the absorbance of which decreases markedly (by c:a 85%) on Ca^{2+}-binding. The exact concentration of the chelator solution (in the range 25–30 μM) was calculated from the absorbance at 239.5 nm in the presence of excess calcium (using $\epsilon_{239.5} = 4.2 \cdot 10^4\ L \cdot mol^{-1} \cdot cm^{-1}$ for quin 2 and $1.6 \cdot 10^4\ L \cdot mol^{-1} \cdot cm^{-1}$ for 5,5′-Br_2-BAPTA). Lyophilized protein was dissolved in the calcium-free chelator solution to obtain a protein concentration of 25–30 μM. The initial total calcium concentration in the protein/chelator solution was determined by atomic absorption spectroscopy, and was in all cases below 2.0 μM. The absorbance at 263 nm (A_{263}) was recorded for the protein/chelator solution. Calcium solution (3.0 mM Ca^{2+} in 2 mM Tris at pH 7.5, with or without 0.15 M KCl) was added in portions of 5 μL using a calibrated Carlsbergh pipette. A_{263} was recorded after each calcium addition. The titration was continued until no absorbance change was seen for the last five additions. Larger calcium additions (5 μL of 10 mM Ca^{2+} in 2 mM Tris at pH 7.5 with 0.15 M KCl) were made at the end of the titrations of the homodimers at 0.15 M KCl. The data analysis has been described in detail elsewhere (Linse et al., 1991). Briefly it consists of computer fitting directly to the measured quantity: absorbance versus total calcium concentration. The initial calcium concentration and the dilutions imposed by calcium additions were taken into account in these fits. The theoretical absorbances were calculated for each set of guessed parameters (K_1, K_2, protein concentration correction factor [F], absorbance in calcium-free solution [A_{MAX}], and the absorbance in calcium-loaded solution [A_{MIN}]) for the total calcium concentrations obtained at the data points. The theoretical absorbances were compared to the measured absorbances to calculate the sum of the squares of residuals, χ^2, which was minimized in an iterative procedure (cf. Linse et al., 1991).

Extra precautions were taken to ensure the stoichiometry of calcium binding to each homodimer. For each individual titration on a homodimer the total protein concentration was measured by amino acid analysis after acid hydrolysis, and the total Ca^{2+} concentration was measured by atomic absorption spectroscopy both before and after the titration. As all calcium additions were made with the same Carlsbergh 5-μL pipette, the total protein

and calcium concentrations at each titration point are thus accurately known. The stoichiometry was obtained as $2 \cdot F$ (cf. Leathers et al., 1990) per dimer.

Five separate experiments were performed for each heterodimer and four for each homodimer. The average value, μ, and standard deviation, σ, of each parameter were calculated as

$$\mu = \sum_{i=1}^{N} (x_i/\alpha_i^2) \Big/ \left(\sum_{i=1}^{N} 1/\alpha_i^2 \right)$$

and

$$\sigma^2 = [1/(N-1)] \sum_{i=1}^{N} [(x_i - \mu)^2/\alpha_i^2] \Big/ \left(\sum_{i=1}^{N} 1/\alpha_i^2 \right),$$

where the x_i's are the values obtained from the individual titrations and N is the number of measurements. The weights ($1/\alpha_i$) used for the values from the individual titrations were evaluated as follows. For example, α_i for $-\Delta\Delta G_{\eta=1}$ in a particular titration was evaluated by doing several computer fits to those titration data points. In each such fit the ratio K_2/K_1 (i.e., $-\Delta\Delta G_{\eta=1}$) was fixed to a selected value, and all other parameters (F, the individual values of K_1 and K_2, A_{MAX}, and A_{MIN}) were allowed to vary to find the lowest possible χ^2 for the selected value of K_2/K_1. The curves of χ^2 versus parameter value (Fig. 5B) are found to be linear above 1.5–2.0 times the χ^2 of the optimal fit (χ^2_{min}). The value of α_i was chosen so that $x_i \pm \alpha_i$ includes the $-\Delta\Delta G_{\eta=1}$ values that give a χ^2 value of $2.0 \cdot \chi^2_{min}$, and α_i can thus be assumed to be proportional to the standard deviation. Error limits α_i for ΔG_{tot} and for F were calculated in the same way. In the evaluation of α_i for ΔG_{tot} the product of K_1K_2 was fixed at a series of values, and in the evaluation of α_i for the individual binding constants, K_1 or K_2 was fixed.

CD method

A protein solution (800 μL; 15–30 μM homodimer) was titrated with Ca^{2+} (5-μL additions of 0.3 mM Ca^{2+} at low ionic strength and 5 μL of 0.3–3 mM Ca^{2+} at 0.15 M KCl). The ellipticity at 222 nm (for cysF1 also at 277 nm) was recorded before the titration and after each Ca^{2+} addition. The measurements at 222 nm monitor the increase in α-helix content on calcium binding, and the measurements on cysF1 at 277 nm utilize the large increase in the CD signal from Tyr 13 on calcium binding. For each individual titration the total protein concentration was measured by amino acid analysis after acid hydrolysis, and the total Ca^{2+} concentration was measured by atomic absorption spectroscopy both before and after the titration. The macroscopic binding constants were obtained from computer fits directly to the data. Analysis of CD data for the case of a protein with only one calcium site is straightforward and is based on the fact that the ellipticity is different in the calcium-free and calcium-loaded forms (Persson et al., 1989). The present analysis is complicated by the fact that we do not know whether the ellipticity for the homodimer with only one calcium ion bound is the same as for the species with two calcium ions bound or the calcium-free species, halfway in between, or something else. In addition, the calcium affinity of each homodimer is so high that curves of cooperative and independent binding show too little difference to allow distinction between these two modes of binding with the present signal-to-noise ratio. The data were analyzed as described by Persson et al. (1989), with the protein concentration set to $f_c \cdot C_{monomer}$, where f_c is a correction factor that was allowed to vary (in addition to the binding constant) to find the optimal fit. The obtained binding constant is a measure of $\sqrt{K_1K_2}$. The stoichiometry of Ca^{2+} binding was obtained as f_c per monomer or $2 \cdot f_c$ per dimer. Standard deviations were evaluated in the same way as for the chelator method.

Urea denaturation

Sets of solutions with different urea concentrations were prepared by mixing appropriate amounts of two stock solutions containing 20 mM PIPES/KOH and either 0 or 9.98 M urea. One set of urea solutions contained 1 mM EDTA and another set contained 1 mM Ca^{2+}. Urea denaturation profiles were obtained by mixing 200 μL of each urea solution with 5 μL of a Ca^{2+}-free protein stock solution, and recording the ellipticity at 222 nm in a 1-mm cuvette. The urea concentration was corrected for the 2.5% dilution on addition of protein. The urea solutions containing EDTA were used for all heterodimers. The Ca^{2+}-containing urea solutions were used for the homodimers. At each urea concentration the ellipticity for the calcium form of the homodimer was first recorded. Then 5 μL of a concentrated EDTA solution was added and the ellipticity for the Ca^{2+}-free form could be recorded for the same homodimer concentration. The latter ellipticity and the urea concentration were corrected for the 2.5% dilution imposed by EDTA addition.

Differential scanning calorimetry

All calorimetric scans were performed with a Microcal MC-2 differential scanning calorimeter. The calorimetric unit was interfaced to a Victor PC computer using an A/D converter board (Data Translation DT-2801) for automatic data collection and analysis. The proteins were dissolved in a 20 mM PIPES, 2 mM EDTA buffer, pH 7.0. Protein concentrations were 500–600 μM (4–5 mg/mL). The scanning rate was 60 °C/h.

Supplementary material

Included on the Diskette Appendix is an almost complete list of assignments for ^1H NMR chemical shifts of $(cysF2)_2 \cdot Ca_2$ at pH 6.0, 27 °C.

Acknowledgments

This work was supported by the Swedish Natural Science Research Council (NFR, K-KU-2545-300). The NMR spectrometer was purchased with generous grants from the Knut and Alice Wallenberg Foundation and the Swedish Council for Planning and Coordination of Research. Comments on the manuscript by Sture Forsén (Department of Physical Chemistry 2, Lund University [DPC/LU]) and Maria Sunnerhagen (DPC/LU) are gratefully acknowledged. We also thank Mats Lundell (DPC/LU) for help with illustrations, and Torbjörn Drakenberg (DPC/LU) and Harald Anderson (Department of Mathematical Statistics, Lund University) for advice on NMR studies and statistical treatment.

References

Akke, M., Forsén, S., & Chazin, W.J. (1991). Molecular basis for cooperativity in Ca^{2+} binding to calbindin D_{9k}. ^1H nuclear magnetic resonance studies of $(Cd^{2+})_1$-bovine calbindin D_{9k}. *J. Mol. Biol. 220*, 173–189.

Brodin, P., Johansson, C., Forsén, S., Drakenberg, T., & Grundström, T. (1990). Functional properties of calbindin D_{9k} mutants with exchanged Ca^{2+} binding sites. *J. Biol. Chem. 265*, 11125–11130.

Cooper, A. & Dryden, D.T.F. (1984). Allostery without conformational change. A plausible model. *Eur. Biophys. J. 11*, 103–109.

Day, C., Schwartz, B., Li, B.L., & Petska, S. (1992). Engineered disulfide bond greatly increases specific activity of recombinant murine interferon-β. *J. Interferon Res. 12*, 139–143.

Dorrington, K.J., Kells, D.I.C., Hitchman, A.J.W., Harrisson, J.E., & Hofmann, T. (1978). Spectroscopic studies on the binding of divalent cations to porcine intestinal calcium-binding protein. *Can. J. Biochem. 56*, 492–499.

Finn, B.E., Kördel, J., Thulin, E., Sellers, P., & Forsén, S. (1992). Dissection of calbindin D_{9k} into two subdomains by a combination of mutagenesis and chemical cleavage. *FEBS Lett. 298*, 211–214.

Grabarek, Z., Tan, R.Y., & Head, J. (1991). Blocking of the Ca^{2+}-induced opening of interhelical interfaces in either of the two domains of calmodulin renders the protein inactive. *Biophys. J. 59*, 23a.

Grabarek, Z., Tan, R.Y., Wang, J., Tao, T., & Gergely, J. (1990). Inhibition of mutant troponin C activity by an intra-domain disulfide bond. *Nature 345*, 132–135.

Habuka, N., Miyano, M., Kataoka, J., Tsuge, H., Ago, H., & Noma, M. (1991). Substantial increase of the inhibitory activity of mirabilis antiviral protein by elimination of the disulfide bond with genetic engineering. *J. Biol. Chem. 266*, 23558–23560.

Johansson, C., Brodin, P., Grundström, T., Thulin, E., Forsén, S., & Drakenberg, T. (1990). Mutation of the pseudo-EF-hand of calbindin D_{9k} into a normal EF-hand. Biophysical studies. *Eur. J. Biochem. 187*, 455–460.

Johansson, C., Ullner, M., & Drakenberg, T. (1993). The solution structures of mutant calbindin D_{9k}'s as determined by NMR show that the calcium binding site can adopt different folds. *Biochemistry 32*, in press.

Kahn, P.C. (1979). The interpretation of near-ultraviolet circular dichroism. *Methods Enzymol. 61*, 339–378.

Kay, L.E., Forman-Kay, J.D., McCubbin, W.D., & Kay, C.M. (1991). Solution structure of a polypeptide dimer comprising the fourth Ca^{2+}-binding site of troponin C by a nuclear magnetic resonance spectroscopy. *Biochemistry 30*, 4323–4333.

Kördel, J., Skelton, N.J., Akke, M.A., & Chazin, W.J. (1993). High resolution solution structure of calcium loaded calbindin D_{9k}. *J. Mol. Biol.*, in press.

Kretsinger, R.H. (1987). Calcium coordination and the calmodulin fold: Divergent versus convergent evolution. *Cold Spring Harbor Symp. Quant. Biol. 52*, 499–510.

Kruse, N., Lehrnbecher, T., & Sebald, W. (1991). Site-directed mutagenesis reveals the importance of disulfide bridges and aromatic residues for structure and proliferative activity of human interleukin-4. *FEBS Lett. 286*, 58–60.

Leathers, V.L., Linse, S., Forsén, S., & Norman, A.W. (1990). Calbindin-D_{28k}, a 1α,25-dihydroxyvitamin D_3-induced calcium-binding protein, binds five or six Ca^{2+} ions with high affinity. *J. Biol. Chem. 265*, 9838–9841.

Linse, S., Brodin, P., Drakenberg, T., Thulin, E., Sellers, P., Elmdén, K., Grundström, T., & Forsén, S. (1987). Structure-function relationships in EF-hand Ca^{2+}-binding proteins. Protein engineering and biophysical studies of calbindin D_{9k}. *Biochemistry 26*, 6723–6735.

Linse, S., Johansson, C., Brodin, P., Grundström, T., Drakenberg, T., & Forsén, S. (1991). Electrostatic contributions to the binding of Ca^{2+} in calbindin D_{9k}. *Biochemistry 30*, 154–162.

Linse, S., Teleman, O., & Drakenberg, T. (1990). Ca^{2+} binding to calbindin D_{9k} strongly affects backbone dynamics: Measurements of exchange rates of individual amide protons using ^1H NMR. *Biochemistry 29*, 5925–5934.

Matsumura, M. & Matthews, B.W. (1991). Stabilization of functional proteins by introduction of multiple disulfide bonds. *Methods Enzymol. 202*, 336–356.

Persson, E., Selander, M., Linse, S., Drakenberg, T., Öhlin, A.-K., & Stenflo, J. (1989). Calcium binding to the isolated β-hydroxyaspartic acid-containing epidermal growth factor-like domain of bovine factor-like domain of bovine factor X. *J. Biol. Chem. 264*, 16897–16904.

Rebek, J., Jr., Costello, T., Marshall, L., Wattley, R., Gadwood, R.C., & Onan, K. (1985). Allosteric effects in organic chemistry: Binding cooperativity in a model for subunit interactions. *J. Am. Chem. Soc. 107*, 7481–7487.

Reid, R.E. (1990). Synthetic fragments of calmodulin calcium-binding site III. A test of the acid pair hypothesis. *J. Biol. Chem. 265*, 5971–5976.

Shaw, G.S., Golden, L.F., Hodges, R.S., & Sykes, B.D. (1991). Interactions between paired calcium binding sites in proteins: NMR determination of the stoichiometry of calcium binding to a synthetic troponin-C peptide. *J. Am. Chem. Soc. 113*, 5557–5563.

Shaw, G.S., Hodges, R.S., & Sykes, B.D. (1990). Calcium-induced peptide association to form an intact protein domain: ^1H NMR structural evidence. *Science 249*, 280–283.

Shaw, G.S., Hodges, R.S., & Sykes, B.D. (1992). Determination of the solution structure of a synthetic two-site calcium binding homodimeric protein domain by NMR spectroscopy. *Biochemistry 31*, 9572–9580.

Skelton, N.J., Kördel, J., Akke, M., & Chazin, W.J. (1992). Nuclear magnetic resonance studies of the internal dynamics in Apo, $(Cd^{2+})_1$ and $(Ca^{2+})_2$ calbindin D_{9k}: The rates of amide proton exchange with solvent. *J. Mol. Biol. 227*, 1100–1117.

Skelton, N.J., Kördel, J., Forsén, S., & Chazin, W.J. (1990). Comparative structural analysis of the calcium free and bound states of the calcium regulatory protein calbindin D_{9k}. *J. Mol. Biol. 213*, 593–598.

Strynadka, N.C.J. & James, M.N.G. (1991). Towards an understanding of the effects of calcium on protein structure and function. *Curr. Opin. Struct. Biol. 1*, 905–914.

Svensson, A., Thulin, E., & Forsén, S. (1992). Proline *cis-trans* isomers in calbindin D_{9k} observed by X-ray crystallography. *J. Mol. Biol. 223*, 601–606.

Szebenyi, D.M.E. & Moffat, K. (1986). The refined structure of vitamin D-dependent calcium-binding protein from bovine intestine. *J. Biol. Chem. 261*, 8761–8777.

Tidor, B. & Karplus, M. (1993). The contribution of cross-links to protein stability: A normal mode analysis of the conformational entropy in the native state. *Proteins Struct. Funct. Genet. 15*, 71–79.

Tsuji, T. & Kaiser, E.T. (1991). Design and synthesis of the pseudo-EF Hand in calbindin D_{9k}: Effect of amino acid substitutions in the α-helical regions. *Proteins Struct. Funct. Genet. 9*, 12–22.

Uchida, E., Uemura, H., Tanaka, T., Nikishawa, S., Uesugi, S., Tanaka, A., Morikawa, M., Hayakawa, T., & Ikehara, M. (1991). Activity of artificial mutant variants of human growth hormone deficient in a disulfide bond between Cys53 and Cys165. *Chem. Pharm. Bull. 39*, 150–153.

Wendt, B., Hofmann, T., Martin, S.R., Bayley, P., Brodin, P., Grundström, T., Thulin, E., Linse, S., & Forsén, S. (1988). Effect of amino acid substitutions and deletions on the thermal stability, the pH stability and unfolding by urea of bovine calbindin D_{9k}. *Eur. J. Biochem. 175*, 439–445.

Wishart, D.S., Sykes, B.D., & Richards, F.M. (1992). The chemical shift index: A fast and simple method for the assignment of protein secondary structure through NMR spectroscopy. *Biochemistry 31*, 1647–1651.

Wüthrich, K. (1986). *NMR of Proteins and Nucleic Acids*. Wiley, New York.